Removal of MAP4 from Microtubules In Vivo Produces No Observable Phenotype at the Cellular Level

Xiao Min Wang,* John G. Peloquin,* Ye Zhai,* J. Chloe Bulinski,‡ and Gary G. Borisy*

*Laboratory of Molecular Biology, University of Wisconsin-Madison, Madison, Wisconsin 53706; and‡Department of Anatomy and Cell Biology, Columbia University College of Physicians and Surgeons, New York 10032

Abstract. Microtubule-associated protein 4 (MAP4) promotes MT assembly in vitro and is localized along MTs in vivo. These results and the fact that MAP4 is the major MAP in nonneuronal cells suggest that MAP4's normal functions may include the stabilization of MTs in situ. To understand MAP4 function in vivo, we produced a blocking antibody (Ab) to prevent MAP4 binding to MTs. The COOH-terminal MT binding domain of MAP4 was expressed in *Escherichia coli* as a glutathione transferase fusion protein and was injected into rabbits to produce an antiserum that was then affinity purified and shown to be monospecific for MAP4. This Ab blocked >95% of MAP4 binding to MTs in an in vitro assay. Microinjection of the affinity purified Ab into human fibroblasts and monkey epithelial cells abolished MAP4 binding to MTs as assayed with a rat polyclonal antibody against the NH_2-terminal projection domain of MAP4. The removal of MAP4 from MTs was accompanied by its sequestration into visible MAP4–Ab immunocomplexes. However, the MT network appeared normal. Tubulin photoactivation and nocodazole sensitivity assays indicated that MT dynamics were not altered detectably by the removal of MAP4 from the MTs. Cells progressed to mitosis with morphologically normal spindles in the absence of MAP4 binding to MTs. Depleting MAP4 from MTs also did not affect the state of posttranslational modifications of tubulin subunits. Further, no perturbations of MT-dependent organelle distribution were detected. We conclude that the association of MAP4 with MTs is not essential for MT assembly or for the MT-based functions in cultured cells that we could assay. A significant role for MAP4 is not excluded by these results, however, as MAP4 may be a component of a functionally redundant system.

THE dynamic character of cytoplasmic organization as displayed in cell locomotion, the interphase–mitosis transition, and the generation of asymmetric cell form prompts consideration of possible mechanisms by which the lability and plasticity of the underlying cytoskeleton might be regulated. Regulation of the microtubule (MT)[1] component of the cytoskeleton, in particular warrants attention because of its central role in determining cell polarity.

Address all correspondence to G. G. Borisy, Laboratory of Molecular Biology, R. M. Bock Laboratories, 1525 Linden Drive, University of Wisconsin-Madison, Madison, WI 53706-1596. Ph.: (608) 262-4570. Fax: (608) 262-4581.

Dr. Wang's present address is Dept. of Molecular Pharmacology, Stanford University School of Medicine, Stanford, CA 94305.

Dr. Zhai's present address is Dept. of Laberatory Medicine, University of California, San Francisco, S.F., CA 94103.

1. *Abbreviations used in this paper*: CLIP, cytoplasmic linker protein; ECL, enhanced chemiluminescence; GST, glutathione S-transferase; IPTG, isopropylthio-β-D-galactopyranoside; MAP, mitogen-activated protein; MPF, maturation-promoting factor; MT, microtubule.

MTs have been demonstrated in vitro to exhibit stochastic alternation between phases of polymerization and depolymerization, a behavior termed dynamic instability (Mitchison and Kirschner, 1984). Similar behavior occurs in vivo (Soltys and Borisy, 1985; Schulze and Kirschner, 1986; Sammak and Borisy, 1988; Cassimeris et al., 1988), although in addition to cycles of growth and shrinking, MTs may also "pause" for some time. While dynamic instability is an intrinsic property of the MT, it is not sufficient to account for regulated changes in cytoskeletal organization. The generation of cell form would seem to require additional factors to spatially or temporally alter MT dynamics.

Microtubule-associated protein 4 (MAPs) have been shown to promote MT polymerization and dampen MT dynamics in vitro (reviewed by Olmsted, 1991; Chapin and Bulinski, 1992; Hirokawa, 1994). Although the biochemical properties of MAPs have been established for some time, their cellular role is as yet not understood. The MAPs originally isolated from brain have been shown to be specific to nervous tissue (MAP2 and tau) or abundant only in nervous tissue (MAP1A and MAP1B). In contrast,

MAP4, originally discovered as a 210-kD MAP in HeLa cells (Bulinski and Borisy, 1979; Weatherbee et al., 1980) has been found in a wide variety of cell and tissue types (Bulinski and Borisy, 1980*b*). Moreover, MAP4 is the principal MAP thus far characterized in proliferating mammalian cells. Cloning and sequencing of MAP4 (human, Chapin and Bulinski, 1991; mouse, West et al., 1991; bovine, also called MAP-U, Aizawa et al., 1990) as well as the neuron-specific MAP2 (Lewis et al., 1988) and tau (Lee et al., 1988) have revealed that all three types of MAP contain, near their respective COOH termini, a shared MT-binding domain containing three to five imperfect repeats of an 18–amino acid motif, an adjacent pro-rich region also involved in MT binding and an NH_2-terminal projection domain. Thus, MAP2, tau and MAP4 constitute a superfamily of MT-binding proteins (reviewed by Bulinski, 1994; Hirokawa, 1994; Matus, 1994).

One attractive hypothesis about the general function of MAPs is that they serve as stabilizers of MTs. Two lines of experimentation have been employed to test the effects of MAPs on MT stability in vivo. One has been to increase the cellular level of MAPs by either transfection or microinjection of protein; the other has been to diminish the level either by the antisense approach or gene targeting. Transfection of both MAP2 and tau into nonneuronal cells or microinjection of tau protein into fibroblasts resulted in enhanced MT stability and assembly as assayed by increased MT polymer number and nocodazole resistance (Drubin and Kirschner, 1986; Lewis et al., 1989; Lee and Rook, 1992). However, Barlow et al. (1994) did not observe that elevated levels of expression of tau or MAP4 increased the MT polymer ratio or stabilized MTs, except for the MT bundles induced by increased tau. The explanation for this discrepancy in results is not clear, although it could be due to different levels of MAP expression or to the use of different cell lines. The results of reductions in MAP2 or tau expression by use of antisense oligonucleotides for tau or MAP2 in cultured neuronal cells have suggested an essential role for these proteins in neurite extension, a process requiring enhanced MT assembly (Caceres and Kosik, 1990; Dinsmore and Solomon, 1991). Yet, a null mutant for tau created by gene targeting yielded mice with no obvious functional defects although the number of MTs was slightly reduced in small caliber axons (Harada et al., 1994). These conflicting results leave the in vivo role of MAPs in MT assembly unresolved.

MT dynamics increase about 20-fold when cells enter mitosis (Saxton et al., 1984). Further, the addition of maturation-promoting factor (MPF) or mitogen-activated protein kinase (MAP kinase) to interphase Xenopus egg extracts increased MT dynamics from interphase to mitotic levels (Verde et al., 1990; Belmont et al., 1990). MAP4 was found to be differentially phosphorylated at the onset of mitosis (Vandré et al., 1991) and in vitro phosphorylation of MAP4 by MPF reduced its MT assembly–promoting activity (Aizawa et al., 1991) and MT-stabilizing ability (Ookata et al., 1995). Shiina et al. (1992) and Anderson et al. (1994) identified 220- and 230-kD MAPs in extracts of Xenopus eggs and suggested on the basis of thermostability and size that they may be related to MAP4. The phosphorylation of these Xenopus MAPs in mitosis reduced their affinity for MTs. Thus, it has been postulated that phosphorylation of MAP4 by mitotic kinase(s) reduces its binding affinity to MTs and modulates the transition from the interphase MT array to the mitotic spindle. This putative reduction in MAP affinity for MTs in mitosis may be taken as another argument that MAPs in interphase serve to stabilize MTs.

The level of MT dynamics in interphase may be considered a constitutive level which can be regulated up or down. In contrast to the majority of spindle MTs, which are more dynamic than the average interphase MT, many cells contain substantial numbers of less dynamic MTs, some of which may survive most of the cell cycle (Schulze and Kirschner, 1987; Webster et al., 1987). The less dynamic MTs are generally marked by posttranslational modifications of the α-tubulin subunits, typically removal of the COOH-terminal tyrosine or acetylation of an ε-amino group of Lys40 (Gundersen et al., 1987; Piperno et al., 1987). However, these modifications appear to be the consequence, not the cause, of the enhanced stability (Khawaja et al., 1988; Webster et al., 1990). Perhaps MAPs, by stabilizing MTs, may indirectly cause MTs to become posttranslationally modified. Indeed, acetylated MTs which correlate with stable MTs have been shown to increase dramatically upon transfection with tau (Lee and Rook, 1992). Related hypotheses for MAP function include roles in regulating the stiffness of MTs and in controlling their spacing (Matus, 1994).

Another possibility for the role of MAPs is that these proteins serve to mediate MT interaction with other organelles within the cell. For example, a MT-binding protein isolated from Hela cells has been demonstrated to be involved in the interaction of endosomes with MTs (Pierre et al., 1992, 1994). This 170-kD protein has been designated a cytoplasmic linker protein (CLIP) and may be one member of a class of MT-interacting molecules.

Because MAP4 is the predominant MAP of nonneuronal cells as well as an ubiquitous component of the MTs of proliferating and differentiating cells, it is likely to be important in a number of MT functions. Thus, to examine the in vivo role of MAP4, we generated a polyclonal Ab against the MT-binding domain of MAP4 in order to block MAP4 binding to MTs in the cell. With this cellular immunodepletion approach, we have tested whether removal of MAP4 altered the MT network, increased MT lability, reduced posttranslational modification, affected mitotic progression, or perturbed the distribution of Golgi and mitochondria.

Materials and Methods

Expression Plasmid Construction

Constructs of MAP4 were derived from the four-repeat species designated isoform III (Bulinski, 1994). The plasmid pGEX-MAP4-C was constructed by inserting a gel-purified 2.0-kb BglII-EcoR1 fragment of the full-length MAP4 isoform Hfb1 (Chapin et al., 1995) into the BamH1 and EcoR1 sites in the multicloning site of pGEX-2T. The protein product of pGEX-MAP4-C (MAP4-C) is a fusion protein with glutathione S-transferase (GST) attached to the NH_2 terminus of the COOH-terminal portion of MAP4 from residue 798. The plasmid pGEX-MAP4-N was constructed by inserting a gel purified 2.4-kb SmaI-NaeI fragment of the plasmid H9454 into the SmaI site in the multicloning site of pGEX-3X. The protein product of pGEX-MAP4-N (MAP4-N) is a fusion protein with GST attached to the NH_2 terminus of an NH_2-terminal portion of

MAP4 up to residue 638. Both plasmids were transformed into *Escherichia coli* strain 11051.

Expression and Purification of MAP4 Proteins

100 ml overnight cultures of transformed cells were diluted to 1 l in LB media supplemented with ampicillin (100 μg/ml) and shaken at 37°C for 45 min. IPTG was added to 0.4 mM and the culture shaken at 22°C for 3 h. Cells were harvested by centrifugation (Sorval GSA rotor, 5,000 rpm, 10 min, 4°C; Dupont Co., Newton, CT) and resuspended in 20 ml of PBS containing 1 N NaCl, 50 mM EDTA, 1 mM PMSF, 10 μg/ml pepstatin A, 10 μg/ml aprotinin. The cells were lysed on ice using a sonicator (Branson Sonic Power, Inc., Danbury, CT), equipped with a microtip, for 6× 1 min at setting 5, and 1% Triton X-100 added before centrifugation (Sorval SS-34 rotor, 30,000 *g*, 40 min, 4°C). The clarified cell extracts were recycled over a 2 ml column of glutathione-Sepharose 4B (Pharmacia, Piscataway, NJ) for 4 h at 4°C. The column was washed with 10 vol of PBS and fusion proteins eluted with 50 mM Tris, pH 8.0, containing 10 mM glutathione. The peak fractions were pooled and dialyzed against PBS at 4°C. The protein concentration was determined by the method of Bradford (Bradford, 1976). It was not possible to usefully cleave the MAP4 fragments from the GST carrier by thrombin digestion because thrombin multiply cleaved the MAP4 domain.

Antibody Production, Purification, and Characterization

Bacterially produced GST-COOH-terminal fusion protein (MAP4-C) was used to immunize New Zealand white rabbits (1 mg per primary injection, 0.5 mg for later boosts). The resulting polyclonal antiserum was affinity purified using purified COOH-terminal fusion protein coupled to Amino-Link Coupling Gel (Pierce Chemical Co., Rockford, IL) following the manufacturer's instructions. After affinity purification, the antibodies were dialyzed against 130 mM KCl, 10 mM Na Pipes, pH 7.0, 1 mM $MgCl_2$ at 4°C, and then concentrated to 6 mg/ml by ultrafiltration using centricon-30 and microcon centrifugal filters (Amicon Corp., Beverly, MA). Affinity purified antibodies were tested for their specificity against human MAP4 by Western blotting. Total Hela extract was separated by 7.5% SDS-PAGE according to the method of Laemmli (1970), transferred to nitrocellulose (Towbin et al., 1979), and probed with the affinity-purified antibody against the COOH-terminal binding domain of MAP4 (anti-MAP4-C) followed by affinity-purified peroxidase conjugated goat anti-rabbit IgG (Kirkegard & Perry Laboratory Inc., Gaithersburg, MD). Antibodies against the NH_2-terminal portion of MAP4 (anti-MAP4-N) were obtained by injecting bacterially expressed and purified GST-MAP4-NH_2-terminal fusion protein into rats (150 μg per primary injection; 100 μg for later boosts). The antiserum was tested for MAP4 specificity as for anti-MAP4-C above.

In Vitro MT Blocking Assay

Pure tubulin was prepared from porcine brain as previously described (Borisy et al., 1975; Vallee and Borisy, 1978). HeLa cell extracts were prepared by brief sonication of cells in PEM buffer (100 mM Pipes, 1 mM EGTA, 1 mM $MgSO_4$, pH 6.9) followed by centrifugation at 150,000 *g* in a TLS-55 rotor (Beckman, Palo Alto, CA) for 20 min at 4°C. Affinity purified antibodies (final concentration 0.6 mg/ml or 0.06 mg/ml) or preimmune IgG (final concentration 0.6 mg/ml) were incubated with the HeLa extract (20 mg/ml) for 1 h at room temperature. After the reaction, tubulin was added (2 mg/ml) in the presence of 10 μg/ml taxol and 1 mM GTP and incubated at 37°C for 15 min to assemble MTs. Finally, the mixture was centrifuged through a cushion of PEM and 20% glycerol at 200,000 *g* in a TLA-100 rotor (Beckman Instruments, Palo Alto, CA) at 20°C for 15 min. The MT pellet was resuspended in PEM buffer containing 0.3 N NaCl and 10 μg/ml taxol. The resuspended solution was spun through PEM buffer and 20% glycerol at 200,000 *g* in a TLA-100 rotor for 15 min at 20°C. The supernatant was analyzed on SDS–polyacrylamide gels and subsequently electroblotted to nitrocellulose (Amersham Corp., Arlington Heights, IL). The blot was incubated with antibodies against the COOH-terminal MT-binding region of MAP4 (anti-MAP4-C) at 2 μg/ml and affinity-purified peroxidase-conjugated goat anti-rabbit antibodies (Kirkegarrd & Perry Laboratories Inc.) diluted to 1:5,000. Peroxidase-labeled antibodies were then detected by incubation of blots with enhanced chemiluminescence (ECL) reagents (1 and 2) and exposure to Hyperfilm (Amersham Corp.).

Quantification of the amount of blocking was done by running a parallel Western blot of different concentrations of total HeLa extract containing known quantities of MAP4 and analyzing as above. The film image was scanned with a Personal Densitometer SI and MAP4 band intensities quantified using ImageQuanNT software (Molecular Dynamics, Sunnyvale, CA).The data for the standard curve of integrated intensity versus concentration of MAP4 was fit by linear regression analysis.

Cell Culture and Microinjection

Human foreskin fibroblasts, line 356 (provided by Dr. Robert DeMars, University of Wisconsin, Madison, WI) and monkey kidney epithelial cells, LLCMK2 (American Type Culture Collection, Rockville, MD) were grown in F-10 medium supplemented with 15 and 5% fetal bovine serum, respectively. For injection, cells were plated onto coverslips with photoetched locator grids (Bellco, Vineland, NJ) and grown for at least 2 d.

Micropipettes were pulled on a vertical pipette puller (Kopf Instruments, Tujunga, CA). The microinjection of Abs was carried out with a Narishige IM-200 microinjector (Greenvale, NY). The needle concentration of microinjected immune and preimmune IgG was 6 mg/ml. For photoactivation studies, since the cells were on the microscope stage for several hours, the temperature was maintained at 37°C with a stage and objective lens heater during the period of the experiment. To prevent pH change, the cell medium was overlaid with mineral oil.

Nocodazole Treatment

Three different experiments were carried out in which cells were treated with nocodazole at different concentrations and for different lengths of time. (*a*) MT lability. To test the lability of MTs in the absence of MAP4, human 356 cells were injected with the affinity purified anti-MAP4-C Ab, and then incubated for 2 h; the cells were treated with nocodazole (0.4 μg/ml) for 5 min, lysed, fixed, and immediately immunostained with antitubulin. (*b*) MT regrowth. LLCMK2 cells were first injected with affinity purified anti-MAP4-C Ab and then incubated at 37°C for 1 h to remove MAP4 from MTs. Nocodazole (4 μg/ml) was added to the medium for 1.5 h (conditions sufficient to depolymerize all tyrosinated (Tyr), detyrosinated (Glu), and acetylated MTs as verified by antitubulin immunostaining). Nocodazole containing medium was removed to allow MT regrowth for 1 h. The cells were then fixed and prepared for immunofluorescence. (*c*) Mitotic collection. LLCMK2 cells injected with the affinity purified anti-MAP4-C were treated with nocodazole at 0.04 μg/ml for 14 h to collect mitotic cells, released from the nocodazole block for 20 min, and then fixed and prepared for immunofluorescence.

Immunofluorescence

For MAP4 staining, cells were fixed with glutaraldehyde followed by lysis with Triton X-100 detergent to avoid the loss of MAP4 from MTs which would result from detergent lysis before fixation (Schliwa et al., 1981). Briefly, cells were washed with PEM buffer at 37°C, immersed in 2% glutaraldehyde for 30 min, and then placed in a permeabilization buffer (0.5% Triton X-100 in PEM buffer) for 15 min. In the experiments in which interphase cells were treated with nocodazole, the cells were lysed with permeabilization buffer for 2 min before fixation with 0.7% glutaraldehyde for 20 min. After fixation, cells were treated with $NaBH_4$ to quench the unreacted glutaraldehyde and blocked with 10% normal goat serum. Primary and secondary Ab incubations were at 37°C for 1 h. The primary antibodies included: NH_2-terminal MAP4 rat polyclonal antiserum at a 1:500 dilution; mouse monoclonal anti-β-tubulin antibody (Amersham Corp.) at a 1:500 dilution for MT staining in interphase cells; YL-1/2 rat monoclonal anti-α-tubulin antibody at a 1:500 dilution in MT regrowth experiments; mouse monoclonal anti-detyrosinated tubulin antibody (undiluted hybridoma cell supernatant; a gift of Dr. J. Wehland, Max-Planck-Institute for Biophysical Chemistry, Heidelberg, Germany), for detyrosinated tubulin staining; mouse monoclonal anti-acetylated tubulin antibody (a gift of Dr. G. Piperno, The Rockefeller University, New York, NY) at a 1:5 dilution for acetylated tubulin staining. The secondary antibodies included: affinity-purified rhodamine-labeled goat anti-rabbit IgG at a 1:100 dilution to stain the injected anti-MAP4-C Ab; affinity-purified fluorescein-conjugated goat anti-rat at 1:50; affinity-purified fluorescein-conjugated goat anti-mouse at 1:50 (Kirkegarrd & Perry Laboratories Inc.).

Images were recorded using either a 100×, 1.3 NA, or a 40×, 1.0 NA objective on an inverted microscope (Zeiss) equipped with a cooled charge-coupled device CCD camera (Photometrics, Tucson, AZ). An Im-

age-1 (Universal Imaging Corp., Westchester, PA) system was used for image processing.

Direct Visualization of MTs, Chromosomes, Mitochondria, and Golgi

For direct visualization of MTs, cells were injected with a mixture of X-rhodamine tubulin (0.6 mg/ml) and anti-MAP4-C IgG (4 mg/ml) followed by fixing and staining as described above. Chromosome staining was done with DAPI at 2 μg/ml for 30 min.

For visualization of mitochondria, the cells were incubated for 10 min in a growth medium containing 10 μg/ml rhodamine 123, a fluorescent dye for selectively staining mitochondria in the living cell (Chen, 1989). For images of the Golgi apparatus in live cells, cells were incubated with the fluorescent lipid analog 6-(*N*-7-nitrobenz-2-oxa-1,3-diazol-4-yl)-ceramide (C_6-NBD-ceramide); 1 μg was dissolved in 850 μl EtOH, and 50 μl was mixed with 10 ml F-10 medium containing 6.8 mg defatted BSA.

Measurements of MT Turnover by Photoactivation

Human 356 cells were injected with affinity purified anti-MAP4-C antibodies and placed at 37°C in a CO_2 incubator for 2 h. A mixture of X-rhodamine tubulin (15 μM) to visualize all MTs and caged-fluorescein tubulin (120 μM) to visualize photoactivated MTs was then injected into the same cells. The cells were allowed to incorporate labeled tubulin subunits into the MTs for at least 1 h before photoactivation and imaging. Photoactivation experiments were performed essentially as described by Zhai et al. (1995).

Results

MAP4 Antibody Production and Characterization

We prepared affinity-purified polyclonal Abs against fusion proteins of GST and segments of human MAP4 containing either the COOH-terminal binding domain (MAP4-C) or the NH_2-terminal projection domain (MAP4-N) expressed in *E. coli.* The MAP4-C binding domain included the MT-binding repeat region and the majority of the proline-rich region (Fig. 1 *A*) both of which have been demonstrated to significantly contribute to MAP4's binding to MTs (Aizawa et al., 1991). SDS-PAGE of the bacterially expressed and glutathione affinity-purified fusion protein (Fig. 1 *B*) shows a principal component of 70-kD apparent molecular weight together with species of lower molecular weight. The apparent molecular weight on SDS gels is higher than the predicted value (GST 27 kD and MAP4-C 34 kD) similar to the behavior of whole MAP4 which has a sequence determined molecular weight of 125 kD but runs at 210 kD. The lower molecular weight bands in Fig. 1 *B* probably represent degradation fragments, since they reacted specifically with an antibody previously characterized as specific for MAP4 (Bulinski and Borisy, 1980*a*). The purified fusion protein was used as immunogen to produce antiserum in rabbits which was affinity-purified on MAP4-C. The results of immunoblotting showed that the affinity-purified antibody (anti-MAP4-C) was specific for MAP4; that is, it recognized a single band comigrating with MAP4 at an apparent molecular weight of 210 kD on a blot of HeLa total protein (Fig. 1 *C*). The expressed and purified MAP4-N projection domain fusion protein migrated on SDS-PAGE predominantly as a single band with an apparent molecular weight of 115 kD (Fig. 1 *B*), again larger than the predicted value (GST 27 kD and MAP4-N 68.6 kD). Antibody produced in rats against the MAP4-N projection domain was specific for MAP4 as assessed by western blotting of HeLa total protein (Fig. 1 *C*).

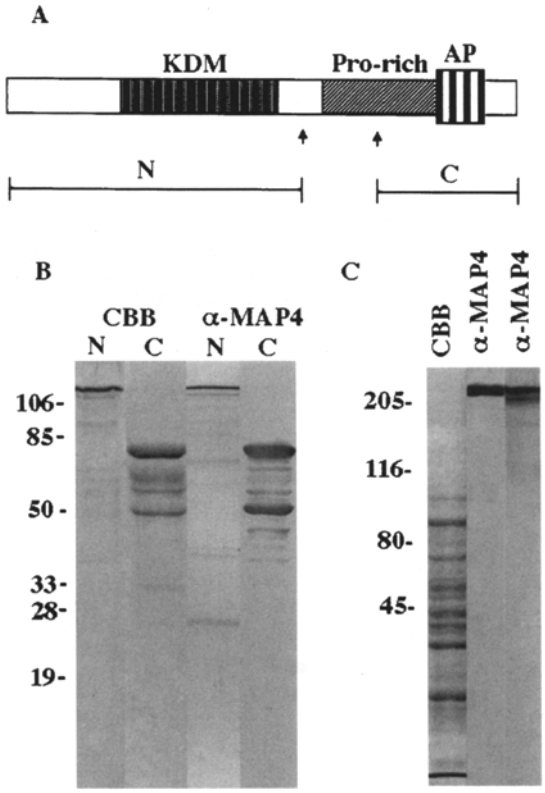

Figure 1. Expression of MAP4 domains and specificity of anti-MAP4 domain Abs. (*A*) Schematic structure of the MAP4 molecule and the MAP4 fragments expressed as GST fusion proteins. Four assembly promoting (*AP*) repeat sequences of 18 residues are indicated by the vertical bars. The proline-rich region (*Pro-rich*) that also contributes to MT binding is indicated by a hatched box. Repetitive motifs of 14 residues (*KDM*) in the amino-terminal domain are indicated by closely spaced vertical lines. The left arrow shows the COOH-terminal boundary of the NH_2-terminal MAP4 domain expressed in the GST fusion protein MAP4-N. The right arrow shows the NH_2-terminal boundary of the COOH-terminal MAP4 domain expressed in the GST fusion protein MAP4-C. The bracketed lines below the arrows indicate the portion of the MAP4 sequence present in MAP4-N (*N*) and MAP4-C (*C*). (*B*) Characterization of bacterially expressed and affinity purified GST–MAP4 fusion proteins. Left two lanes show *E. coli* expressed glutathione affinity purified GST-MAP4 proteins electrophoresed on a 10% SDS–polyacrylamide gel and stained with Coomassie brilliant blue dye (*CBB*). Right two lanes show immunoblotting of *E. coli* expressed glutathione affinity purified GST-MAP4 proteins with a polyclonal antibody generated against the whole MAP4 molecule (*α-MAP4*; Bulinski and Borisy, 1980*a*). *N*, MAP4-N; *C*, MAP4-C. Molecular weight markers are indicated at left. (*C*) Characterization of antibodies specific for the MAP4 binding and projection domains. Total Hela extract was electrophoresed on 10% SDS–polyacrylamide gel and stained with Coomassie brilliant blue (*CBB*). A Western blot of the total Hela cell extract was probed with affinity purified rabbit antibody to the MAP4 MT binding domain (anti-MAP4-C), and with rat antiserum raised against the MAP4 projection domain (anti-MAP4-N). The reactive bands were visualized with peroxidase-conjugated secondary antibodies and enhanced chemiluminescence (*ECL*) reagents. Molecular weight markers are indicated.

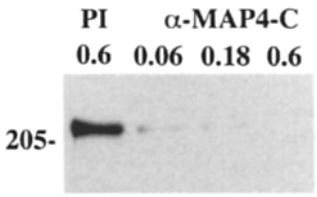

Figure 2. In vitro antibody blocking of MAP4 binding to microtubules. Western blots showing inhibition of MAP4 binding to MTs in HeLa extracts. Extracts were pre-incubated with pre-immune IgG or anti-MAP4-C IgG. The final supernatant fraction from the blocking assay containing MAPs extracted from MTs with 0.3 N NaCl was separated by 7.5% SDS-PAGE, electroblotted to nitrocellulose, and probed with anti-MAP4-C IgG and peroxidase conjugated secondary antibody and visualized with ECL reagents. *PI* (0.6), pre-immune IgG (0.6 mg/ml); *α-MAP4-C* (0.06), anti-MAP4-C IgG (0.06 mg/ml); *α-MAP4-C* (0.18), anti-MAP4-C IgG (0.18 mg/ml); *α-MAP4-C* (0.6), anti-MAP4-C IgG (0.6 mg/ml). Molecular weight markers are indicated.

The Ab against the Binding Domain Blocks MAP4 Binding to MTs In Vitro

To test whether the anti-MAP4-C Ab could block MAP4 binding to MTs in vitro, we devised an assay to measure blockage of MT binding. HeLa cell extracts containing MAP4 were preincubated with varying concentrations of purified anti-MAP4-C. Tubulin was then added in sufficient quantity to produce a great excess of MAP-binding sites when polymerization was induced with taxol. The MTs were sedimented through a glycerol cushion to separate MAP4 bound to MTs from free MAP4. We found that MAP4–anti-MAP4-C complexes sedimented in the absence of MTs. Therefore, MT-bound MAP4 was extracted from the MTs with 0.3 N NaCl and separated from the MTs and MAP4–Ab complexes by sedimentation. The final supernatants were analyzed for MAP4 content by Western blot. Anti-MAP4-C blocking of MAP4 binding to MTs was assayed as a decrease in MAP4 relative to a preimmune IgG control. As shown in Fig. 2, the level of MAP4 bound to MTs decreased to nearly undetectable levels with increasing anti-MAP4-C IgG concentration. A quantitative assessment of the reduction of MAP4 binding (see Materials and Methods) demonstrated that MAP4 binding to MTs was reduced by 85% in the presence of 0.06 mg/ml anti-MAP4-C Ab, 94% with 0.18 mg/ml antibody, and by 98% at an antibody concentration of 0.6 mg/ml.

Removal of MAP4 from MTs by Ab Injection

Similar to the results obtained previously for Abs against whole MAP4 purified from Hela cells by Bulinski and Borisy (1980*a*), our anti-MAP4-C Ab showed strong cross-reactivity only with MAP4 from humans and other primates (data not shown). Therefore, we chose human 356 cells (primary fibroblasts) and monkey LLCMK2 cells (kidney epithelia) for microinjection. Cells were injected with Ab at a needle concentration of 6 mg/ml and at a volume estimated from previous studies in the laboratory to be 5–10% of the cell volume. Assuming the same effectiveness of the antibody in vivo as in vitro, the resulting concentration in the cells would approach levels sufficient for almost complete blocking of MAP4 binding to MTs. The cells were then incubated for various periods of time and prepared for immunolocalization of MAP4. Because it was difficult to find cells several hours after injection due to cell movement, the cells were also labeled with goat anti–rabbit Abs to distinguish injected cells from noninjected ones. This label also allowed us to assay the relative

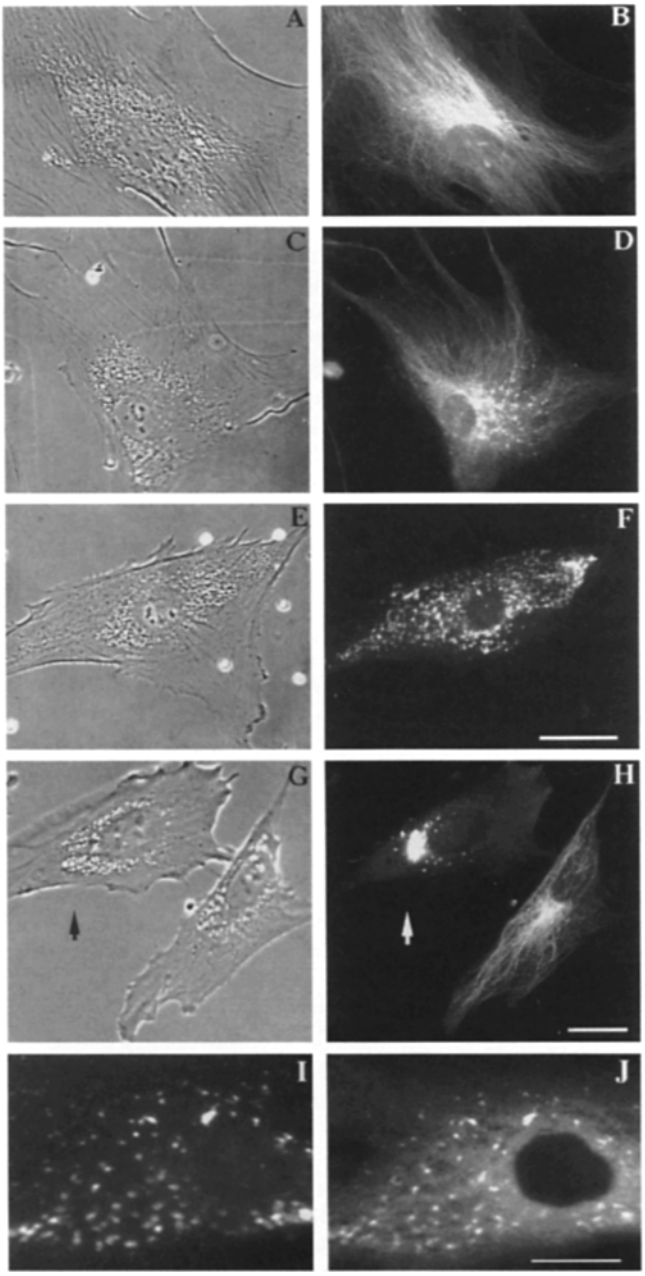

Figure 3. Time course of removal of MAP4 from MTs in cells. Human 356 cells were injected with either preimmune IgG (6 mg/ml) (*A* and *B*) or affinity-purified anti-MAP4-C IgG (6 mg/ml) (*C–H*). The control cell (*A* and *B*) was fixed 2 h after the injection of preimmune IgG; The cells injected with anti-MAP4-C were fixed: 1 h (*C* and *D*), 2 h (*E* and *F* and *I* and *J*), and 24 h (*G* and *H*) after injection. All cells were stained with rat anti-MAP4-N serum and with fluorescein-labeled goat anti–rat antibodies to reveal the distribution of MAP4 (*B*, *D*, *F*, *H*, and *I*). The cell in *I* and *J* was also stained with rhodamine-labeled goat anti–rabbit IgG to show the distribution of injected Ab. Phase micrographs, (*A*, *C*, *E*, and *G*). (*G* and *H*) Pair of cells, only one of which was injected with the anti-MAP4 C (*arrows*). Bars: (*A–F*) 20 μm; (*G* and *H*) 15 μm; (*I* and *J*) 10 μm.

amount of Ab injected. Anti-MAP4-N stained MTs strongly in preimmune injected or uninjected cells (see below, Fig. 3, *A* and *B*). In contrast, anti-MAP4-C stained MTs in fixed cells very weakly (data not shown), perhaps because the MAP4-binding domain epitopic sites were not accessible when associated with MTs. Since MAP4 binding to MTs has been demonstrated to be highly dynamic in vivo (Olmsted, 1989), we reasoned that in live cells the injected Abs would have ample opportunity to interact with MAP4 during its dissociation from MTs. After Ab injection, loss of MAP4 binding to MTs was a gradual process as could be seen by the changes in the distribution of MAP4 revealed with the antibody directed against the NH_2-terminal projection domain of MAP4 (Fig. 3). At 1 h after the injection of anti-MAP4-C, MAP4 was only partially removed from MTs, and both MT staining and weak spots could be seen. By 2 h after injection, MAP4 staining of MTs was not detectable and bright spots were seen throughout the cytoplasm. The injected anti-MAP4 visualized with anti–rabbit IgG staining (Fig. 3 *J*) was visible as bright spots superimposed on a diffuse distribution of Ab, suggesting an excess of Ab in the cytoplasm. The anti-MAP4-C spots colocalized with the MAP4 spots (Fig. 3, *I* and *J*) indicating that the spots comprised an immunoprecipitation complex of MAP4 and anti-MAP4-C. With longer incubation, the MAP4 aggregates increased in size and after 24 h, only one or a few large MAP4 aggregates were present. MAP4 staining of MTs remained below detectable levels for more than 24 h indicating that sequestration of MAP4 by the antibody was essentially irreversible. Injection of pre-immune IgG did not affect the normal distribution of MAP4 on the MTs indicating that the blocking effect was a specific property of anti-MAP4-C.

Effects of Removal of MAP4 from MTs on In Vivo MT Assembly and Organization

Previous evidence indicated that MAP4 promotes MT assembly in vitro (Bulinski and Borisy, 1980*c*; Aizawa et al., 1991). Therefore, we tested whether cells injected with anti-MAP4-C Abs retained the normal distribution and density of the MT network. Remarkably, despite the fact that MAP4 staining of MTs was no longer detectable, anti-tubulin MT staining (Fig. 4 *C*) demonstrated that both the MT network and the density of MTs appeared indistinguishable from noninjected control cells (Fig. 4 *A*). The high magnification view of an anti-MAP4-C–injected cell shows no anti-MAP4 labeling of MTs (Fig. 4 *F*) although individual MTs are clearly resolved with anti-tubulin staining (Fig. 4 *E*). The normal organization of MTs was maintained for at least 24 h after the injection (not shown) despite the seemingly irreversible sequestration of MAP4 by Ab. No obvious changes were seen in the linearity, curvature or distribution of the MT network suggesting that no large modifications had occurred in either the stiffness of the MTs or in their tendency to remain separate rather than bundled under normal growth conditions. Retention of the MT network suggested that removal of MAP4 did not reduce MT assembly.

To examine possible changes in MT stability with greater sensitivity, we used the MT depolymerizing drug nocodazole under conditions designed to dramatize differences in MT lability. One of a pair of sister cells was injected with anti-MAP4-C followed by nocodazole treatment previously shown to depolymerize about one half of the original MTs in the noninjected cells (data not shown). Sister cells were chosen as they yield a more accurate comparison than cells randomly chosen from the general population. As shown in the example in Fig. 5, no noticeable difference in MT density was observed between the injected and noninjected sister cells.

Since it is possible that MAP4 is involved in the formation of the MT network, but is no longer needed once the array has formed, we tested the capacity of cells to regrow MTs after release from nocodazole treatment. We again took the approach of injecting one cell in a pair of sister cells with anti-MAP4-C Ab. LLCMK2 cells were treated with nocodazole at 4 μg/ml for 1.5 h, under which conditions all the MTs were depolymerized (data not shown). Subsequently, the nocodazole was removed and the cells were reincubated for 1 h to allow regrowth of MTs. Fig. 5 shows a representative pair of sister cells with similar mor-

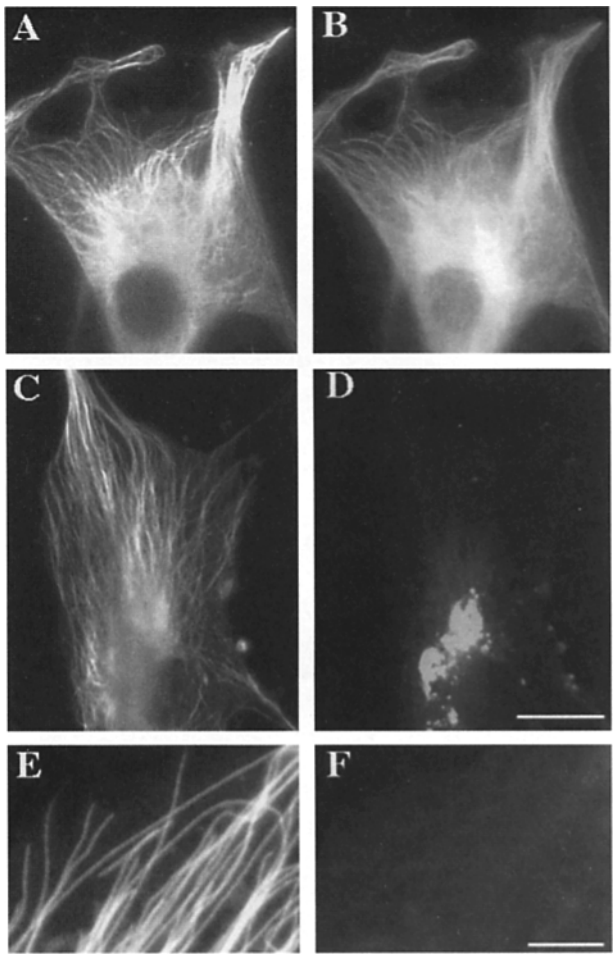

Figure 4. The microtubule network appeared unaffected by removal of MAP4. Human 356 cells double immunofluorescently labeled for tubulin (*A*, *C*, and *E*) and MAP4 (*B*, *D*, and *F*). The uninjected cell (*A* and *B*) shows colocalization of tubulin and MAP4. (*C–F*) Cells were injected with affinity-purified anti-MAP4-C (6 mg/ml) and fixed 4 h later. MAP4 localization on MTs is no longer detectable. Bars: (*A–D*) 20 μm; (*E* and *F*) 10 μm.

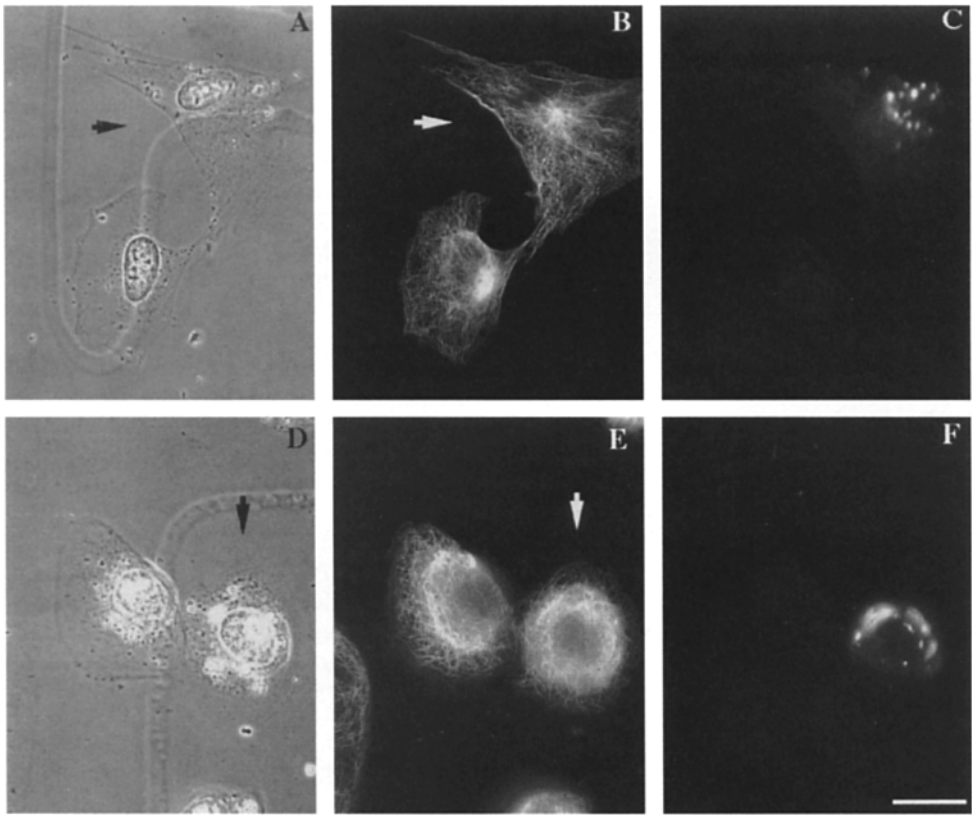

Figure 5. Microtubules are not rendered hyper-labile by removal of MAP4 and can regrow in the absence of MAP4. Sister cells early in G1, as identified by a residual midbody, were used to test lability of microtubules to nocodazole-induced depolymerization and capacity for microtubule regrowth. One cell of each pair of sister cells was injected (*arrows*). (*A–C*) Human 356 fibroblast injected with anti-MAP4-C Ab (6 mg/ml), and 2 h later treated with nocodazole (0.4 μg/ml) for 5 min to depolymerize about 50% of the MT polymer, followed by lysis and fixation and staining by anti-tubulin antibody (*B*). (*D–F*) LLCMK2 cell injected with anti-MAP4-C and 2 h later treated with nocodazole (4 μg/ml) for 1.5 h to depolymerize all the MTs and then allowed to regrow MTs for 1 h in nocodazole-free medium. Finally, the cell was lysed, fixed, and stained with anti-tubulin antibody (*E*). Rhodamine-labeled goat anti–rabbit antibodies were used to visualize the injected antibodies, confirming the identity of the injected cells (*C* and *F*). Since the cells were lysed first to remove the soluble tubulin in order to reduce the background, there is little diffuse fluorescence seen in the goat anti–rabbit IgG panels (*C* and *F*). Bars: 20 μm (*A–C*); 15 μm (*D–F*).

phologies and MT distributions. This result indicates that MTs can regrow in the absence of detectable MAP4 binding.

Finally, MT dynamics were evaluated using photoactivation of injected caged fluorescein. The fluorescence dissipation curves showed no significant difference between the two cell populations, demonstrating quantitatively that MAP4 removal did not alter MT turnover rates (Fig. 6). Thus, three different assay procedures failed to show an effect of MAP4 removal on microtubule organization, assembly or stability.

Posttranslational Modifications of Tubulin Are Not Affected by Removal of MAP4 from MTs

We also tested the role of MAP4 in MT dynamics and function by examining the subset of stable MTs marked by posttranslational modifications in MAP4-depleted and control cells. MAP4 could be involved in the acquisition of those modifications either directly or indirectly. A direct involvement would suggest that MAP4 participated in the posttranslational modification system. An indirect involvement might result from a stabilizing effect of MAP4 on MTs, since posttranslational modifications have been demonstrated to be a consequence rather than a cause of stability (Khawaja et al., 1988; Webster et al., 1990). Although in our previous experiments the MT array was not altered by blocking of MAP4 binding to MTs, a MT subset might have been altered.

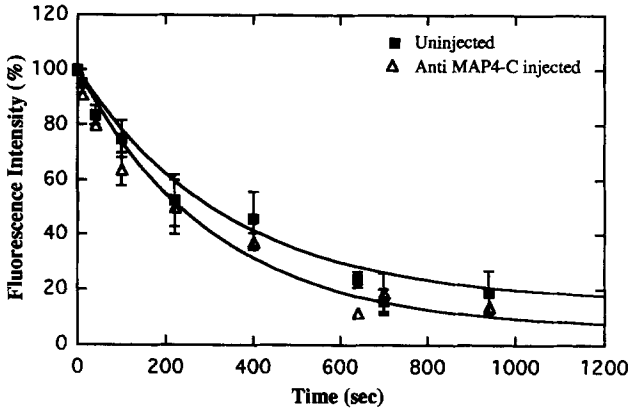

Figure 6. Microtubule turnover is not measurably altered by removal of MAP4. Cells were injected with anti-MAP4-C and incubated for 2 h to allow removal of MAP4. The same cells were injected a second time, and this time with a mixture of x-rhodamine tubulin to visualize microtubules and caged-fluorescein tubulin for analysis of microtubule dynamics by redistribution of fluorescence after photoactivation. Cells were photoactivated as described in Materials and Methods. The time course of fluorescence redistribution after photoactivation was plotted as a percentage of fluorescence intensity remaining in the activated zones. △, Cells injected with anti-MAP4-C (n = 7, mean ± SD); X, control cells (n = 7, mean ± SD).

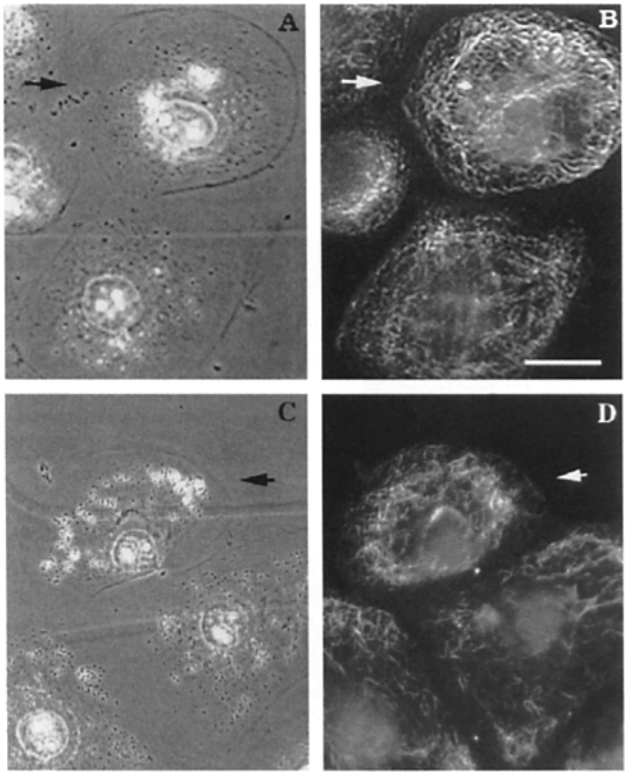

Figure 7. Post-translational modification of tubulin is unaffected by removal of MAP4. Sister cells were used as described in Fig. 5 with one being injected (*arrows*) and one serving as the control cell (*A* and *C*). LLCMK2 cells were injected with affinity-purified anti-MAP4-C IgG (6 mg/ml) first, and 2 h later treated with nocodazole (4 μg/ml) for 1.5 h to depolymerize all the MTs, including detyrosinated MTs and acetylated MTs (not shown). Then, they were washed free of the drug to allow MT regrowth for 1 h. Finally, the cells were lysed, fixed and stained with detyrosinated tubulin antibody (*B*) and acetylated tubulin antibodies (*E*) respectively. No obvious differences in the staining patterns were seen. Bar, 15 μm.

To examine the effect of depletion of MAP4 on the level of posttranslational modification of MTs, we compared injected versus noninjected cells stained with Abs against detyrosinated or acetylated tubulin. We conducted MT regrowth experiments as described previously, because these modifications are alterations at the MT polymer level, i.e., postpolymerization (Gundersen et al., 1987). Cells were treated with nocodazole to depolymerize all the detyrosinated and acetylated MTs (data not shown). Nocodazole was then removed, allowing the resultant pool of tubulin monomer to polymerize and subsequently gain posttranslational modifications. MAP4 staining of MTs was absent in Ab injected cells throughout this time course. No significant difference in detyrosinated or acetylated MTs was seen in injected versus uninjected cells (Fig. 7) suggesting that the array of posttranslationally modified MTs was not dependent on the presence of MAP4 on MTs.

Depletion of MAP4 on MTs Did Not Prevent Mitotic Progression

To evaluate the dependence of spindle formation and function on MAP4, we examined whether MAP4 could be depleted from mitotic spindles as well as from interphase MTs. We microinjected MAP4-C Ab into LLCMK2 cells in interphase and treated them with a low concentration of nocodazole (0.04 μg/ml) in order to accumulate mitotic cells. The cells were released from nocodazole and fixed when the majority had progressed to metaphase. As seen in Fig. 8 *B*, MAP4 was not localized on spindles in the injected cells; instead, large MAP4-containing aggregates were present. To discern whether a normal mitotic spindle could form in cells depleted of MAP4, we microinjected cells with a mixture of rhodamine-labeled tubulin and anti-MAP4-C and treated them as above using the incorporated rhodamine-labeled tubulin to visualize spindle formation. As seen in Fig. 8 (*D–F*), spindle morphology was normal even though MAP4 was not detectable on spindle MTs.

To determine if cells were capable of division with MAP4 depleted from MTs, LLCMK2 cells were injected in interphase with anti-MAP4-C and followed for 24 h. The cells were fixed and stained with rat polyclonal antibodies against the NH_2-terminal portion of MAP4 (anti-MAP4-N). Most of the cells divided within one cell cycle. Cytokinesis and reconstitution of the interphase MT network after division both appeared to be normal; although no MAP4 staining was seen on MTs (Fig. 9 *B*), the MT array reformed normally (Fig. 9 *D*). Our results suggest that MAP4 is not essential for progression through mitosis and into G_1.

Microtubule-dependent Intracellular Organelle Distribution Was Not Affected by Removal of MAP4 from MTs

Organization and cellular positioning of the Golgi is dependent upon MTs, as demonstrated by the fragmentation of the Golgi in interphase cells with drug-induced disruption of MTs. Perturbations of Golgi distribution also occur normally when the Golgi fragments at the onset of mitosis (Allan and Kreis, 1986). Likewise, mitochondria typically coalign with MTs in fibroblasts and their distribution depends on the integrity of the cytoplasmic MT network (Ball and Singer, 1982). To test whether MAP4 mediates the interaction of MTs and these membranous organelles, we performed assays of the distribution of both Golgi and mitochondria in cells in which MTs were depleted of MAP4 by Ab injection.

We used C_6-NBD-ceramide, a fluorescent lipid derivative, to stain the Golgi apparatus (Pagano, 1989) and the fluorescent dye, rhodamine 123, to stain the mitochondria of living cells (Chen, 1989), that had been injected with anti-MAP4-C Ab and incubated for 2 h. As shown in Fig. 10 (*A* and *B*), the congregation of the Golgi apparatus around the centrosome was not altered in cells in which MAP4 was depleted from MTs. Likewise, mitochondria formed long filaments extending to the tip of the cell process indicating alignment along MTs (Fig. 10, *C* and *D*), indicating there was no perturbation of the distribution of mitochondria in anti-MAP4-C–injected cells. Thus, removal of MAP4 from microtubules failed to show an effect on the distribution of either of two kinds of cellular organelle.

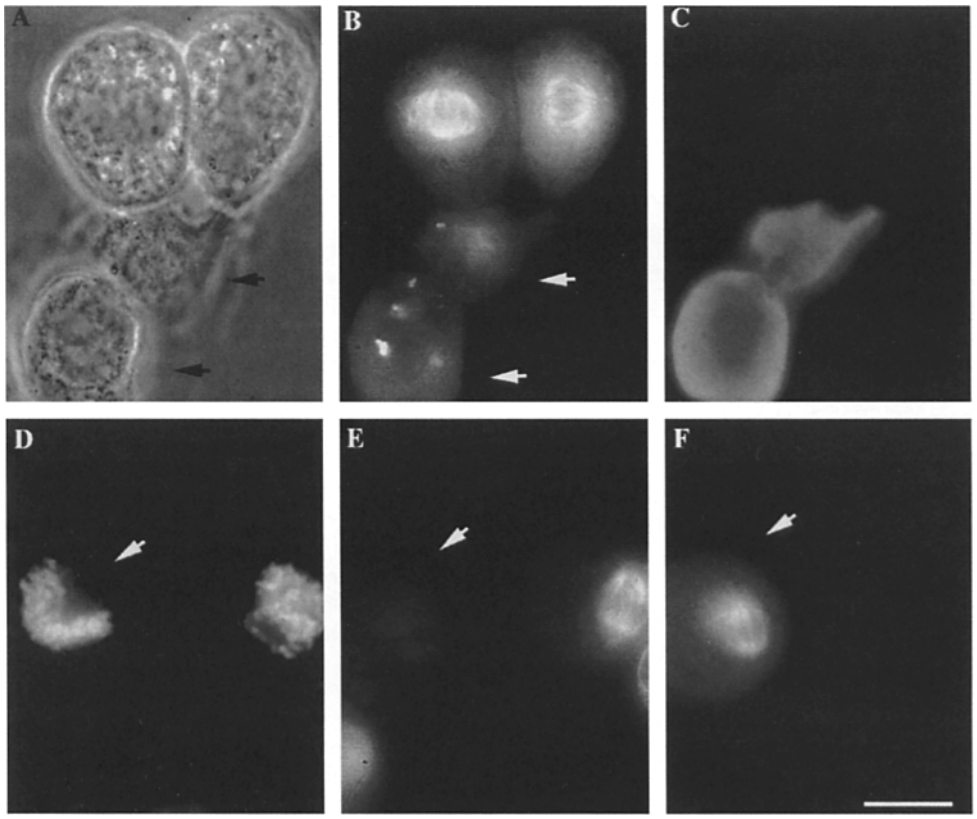

Figure 8. Spindle formation and mitosis proceed in the absence of MAP4. (*A–C*) Group of four mitotic cells collected by treatment with nocodazole at low concentration (0.04 μg/ml) for 14 h. (*A*) Two cells were injected with anti-MAP4-C IgG (6 mg/ml) in interphase (*top*) and two cells were not injected (*bottom*). After removal of nocodazole, the cells were allowed to progress for 20 min before being fixed and processed for immunofluorescence. Arrows point to the injected cells. (*B*) Immunostaining with anti-MAP4-N Ab shows spindle structures in the uninjected cells whereas injected cells show MAP4 immunoprecipitation aggregates and an absence of spindle staining. (*C*) Rhodamine labeled goat anti–rabbit staining confirms the identity of the injected cells. (*D–F*) show a cell (*arrow*) injected with a mixture of x-rhodamine–labeled tubulin (0.6 mg/ml) and anti-MAP4-C IgG (0.4 mg/ml) and treated with nocodazole as for the cells in *A–C*. (*D*) Cells stained with DAPI to show condensed chromosomes in two cells, left and right; (*E*) immunostaining with anti-MAP4-N Ab shows no reactivity in the injected cell (*left, arrow*) but a normal spindle in the uninjected cell (*right*); (*F*) direct fluorescence image of x-rhodamine–tubulin incorporated into the spindle of the injected cell confirms that a normal spindle was formed in the absence of MAP4. Bar, 20 μm.

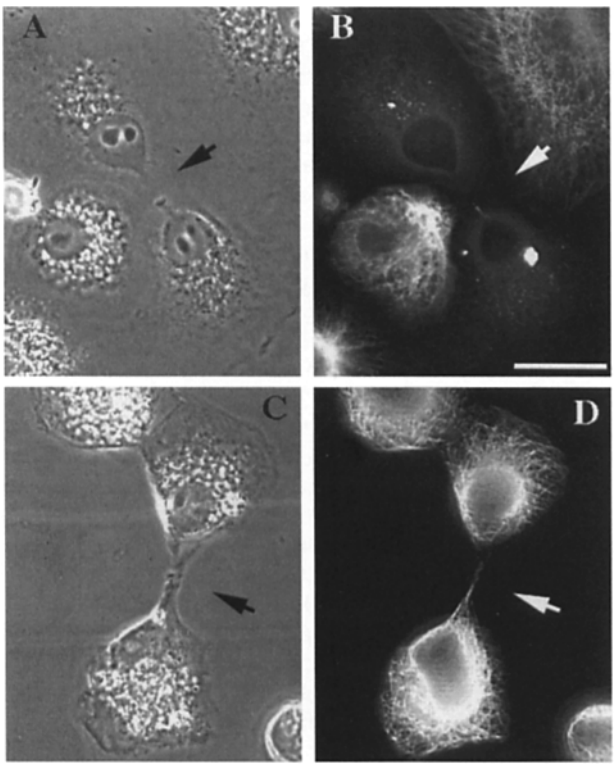

Discussion

Our results demonstrate that an affinity-purified polyclonal Ab against the MAP4 COOH-terminal region is effective in blocking binding of MAP4 to MTs in vitro and in vivo. Remarkably, the removal of MAP4 from MTs in vivo produced no observable phenotype at the cellular level. Because of this apparently negative result, it is important to consider the efficiency of removal of MAP4 and whether low levels of MAP4 would be sufficient to maintain cellular function. Qualitatively, the absence of MAP4 staining of mitotic spindles in which MTs are highly concentrated would suggest MAP4 removal was very efficient. A quantitative assessment of the degree of MAP4 removal from MTs in vivo was not feasible, since the MAP4 staining of cells is not reduced by Ab blocking; instead, the

Figure 9. Cell cycle progression, completion of mitosis and cytokinesis in the absence of MAP4. Cells were injected with anti-MAP4-C antibodies as single cells in interphase and returned to culture for 24 h. (*A* and *C*) The injected cells have divided into two sister cells, identifiable by the residual midbody. (*B*) Immunostaining with anti-MAP4-N Ab indicates an immuno-aggregate of MAP4 in each sister cell but absence of MAP4 staining of microtubules. (*D*) Antitubulin staining indicates that microtubules remained intact. Bar, 20 μm.

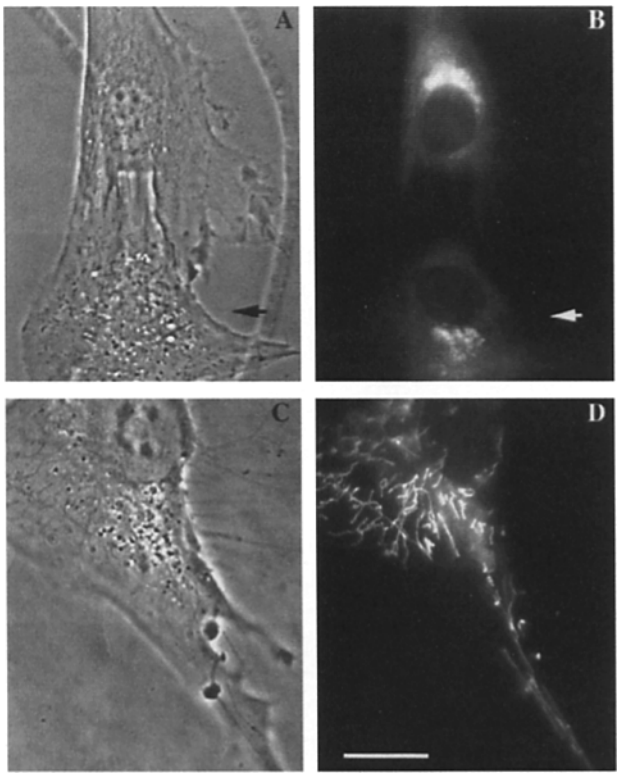

Figure 10. The distribution of Golgi and mitochondria in MAP4 immuno-depleted cells. (*A* and *B*) A pair of sister cells, one of which was injected with anti-MAP4-C Ab (*arrows*); (*B*) Staining with C_6-NBD-ceramide for Golgi indicates that the Golgi apparatus remains compact and in the perinuclear area in injected as well as uninjected cells. (*C* and *D*) Cell injected with anti-MAP4-C Ab. (*D*) Staining with rhodamine 123 for visualization of mitochondria in the living cell indicates that mitochondria remain dispersed throughout the cytoplasm in injected as well as uninjected cells. Bar, 15 μm.

staining is relocated from MTs to MAP4–Ab aggregates. Although our blocking assay conditions in vitro may not be exactly comparable to the in vivo situation, the levels of blocking observed in vitro provide a reasonable estimate of the range of blocking efficiency achievable by anti-MAP4-C microinjection. In vitro, MAP4 removal was 85% at a concentration of 0.06 mg/ml Ab (equivalent to injection of 1% of the cell volume with Ab at a needle concentration of 6 mg/ml) to 98% at a concentration of 0.6 mg/ml (equivalent to injection of 10% of the cell volume with 6 mg/ml Ab). The mass ratio of MAP4 to tubulin monomer in Hela cell extracts was previously estimated as 1% (Bulinski and Borisy, 1980*a*). Assuming 2/3 of tubulin is in the form of polymer (Zhai and Borisy, 1994) and greater than 90% of MAP4 is bound to MTs (Bulinski and Borisy, 1980*a*) and given the molecular weight for MAP4 of 125,000 and for tubulin monomer of 50,000, this corresponds to a molar ratio of MAP4 to tubulin monomer on the microtubule of 1:185. If blocking was 85–98% efficient in vivo, the remaining MAP4 would be at a 1:1,240–1:9,250 ratio to tubulin monomer. Given that the MT lattice contains 3,650 tubulin monomers per μm length, this would mean the residual MAP4 would be at a level of less than one to three molecules per μm. This level would likely be below detection limits by conventional immunofluoresence. We cannot exclude the possibility that such a small amount of remaining MAP4 might be enough to maintain its functions; however, were such a small amount to be sufficient, it would mean that the cell normally produces a 7–50-fold surplus of MAP4, a biologically improbable condition.

A previous investigation using a monoclonal Ab against only the third assembly promoting repeat of MAP2 found no inhibition of MAP binding to MTs (Dingus et al., 1991). Instead the Ab bound to the MAPs and co-sedimented with MTs. Our polyclonal antiserum, which was raised against a COOH-terminal domain of MAP4, presumably contains a number of different antibody species whose epitopes span the MT-binding region. This allows for two blocking mechanisms which are not possible with a monoclonal IgG directed against a single epitope: (*a*) Ab binding to multiple MAP epitopes in the MT-binding region producing steric inhibition of binding; (*b*) formation of Ab-MAP immunoprecipitates which irreversibly sequester MAPs. Both the ability to sediment the MAP4–Ab complexes in our in vitro assay and the formation of MAP4 containing aggregates in the anti-MAP4–injected cells would suggest that removal of MAP4 from MTs is ultimately a result of its sequestration in immunoprecipitates. Initially, the Abs could either interact with epitopes at the MT binding site and thus displace MAP4 and/or interact with MAP4 in the soluble pool and prevent its rebinding to MTs. Because MAP4 binding to MTs was determined to be in rapid equilibrium with a half life of about 44 s in interphase cells (Olmsted et al., 1989), binding of Ab to MAP4 molecules in the soluble pool would be expected to drive the equilibrium away from the MT-bound state, thus depleting the MTs of MAP4.

Immunoprecipitation of cytoskeletal proteins within live cells following microinjection of specific polyclonal Abs has been observed previously for nonerythrocyte spectrin (Mangeat et al., 1984), α-actinin (Jockusch, 1991), and talin (Nuckolls et al., 1992). Cells in which the antigen has been quantitatively precipitated (as assessed by immunofluorescence) have been characterized as "phenotypically equivalent to mutants defective in their (cytoskeletal protein)" (Mangeat et al., 1984).

Injection of anti-MAP4-C into cells effectively removed MAP4 from MTs, constituting an in vivo immunodepletion experiment. Yet, unexpectedly, no effect on MT stability or assembly was observed. The ability of MAPs, including MAP4 to promote MT assembly and affect MT dynamics is well characterized in vitro (reviewed by Hirokawa, 1994). Based on these in vitro studies, it was reasonable to expect that MTs depleted of MAP4 would exhibit abnormalities. However, a review of attempts to modulate MAP levels in vivo indicates that the results available to date are enigmatic. On one hand, a number of studies have demonstrated that MT stability and increased tubulin assembly correlate with the introduction of exogenous MAPs. Injection of tau protein, at a level predicted to be sufficient to saturate its MT-binding sites, led to a 44% increase in MT polymer as well as resistance of MTs to depolymerization by nocodazole (Drubin and Kirschner, 1986). Transfection of nonneuronal cells with the neu-

ronal MAPs, tau, MAP2 or MAP2c, at high levels of expression, resulted in the formation of MT bundles with greatly enhanced stability (Lewis et al., 1989; Kanai et al., 1992; Lee and Rook, 1992). On the other hand, injection of fluorescein-derivatized MAP2 or MAP4 at concentrations comparable to endogenous levels produced no discernible difference in the amount of MT polymer or MT stability (Vandenbunder and Borisy, 1986; Olmsted et al., 1989). In a recent report, Barlow et al. (1994) did not observe a significant effect on MT polymer level or drug stability in stable CHO cell transfectants that expressed high levels of MAP4 or tau.

Investigations designed to elucidate MAP functions by reduction of MAP expression have similarly yielded similarly mixed results. Lowering tau expression with antisense oligonucleotides indicated that tau was required for the development of MT-containing axon-like processes in cultured cerebellar cells (Caceres and Kosik, 1990). MAP2 antisense constructs were used to inhibit MAP2 expression and showed that cells induced to differentiate into neurons lacking MAP2 cannot extend neurites (Dinsmore and Solomon, 1991). These studies suggested that MAP expression may be essential in producing the increased level of highly stabilized MTs characteristic of mature neurons. However, targeted mutation of the tau gene to produce mice that lacked tau expression resulted in only a subtle structural alteration in one type of cerebellar axon, and the mice suffered no functional consequences. Further, Drosophila bearing a homozygous deficiency for the 205-kD MAP gene were fully viable and showed no obvious phenotype (Pereira et al., 1992). These different results leave open the question of MAP function in cells and in animals.

Both overexpression and deletion experiments have intrinsic limitations. A general problem for overexpression studies is their relevance to function at normal levels. Artifacts of mislocalization, artifacts due to occupancy of low affinity binding sites, or in the case of MAPs, MT bundle formation may occur. On the other side, overexpression of a MAP might yield no phenotype if either the overexpressed protein or MT dynamic parameters are regulated to resist changes which might result from increased expression. Deletion experiments in whole organisms may also be hard to interpret because other proteins might overlap the function of the deleted protein. For example, the mice in which tau was knocked out showed higher levels of MAP1A (Harada et al., 1994); perhaps their level of MAP4 (which was not assayed) was also changed. Although compensatory mechanisms may exist at either the organismal or cellular levels, we consider that studies directed at the cellular level often provide a more direct way of assaying cellular function. Further, higher resolution assays are available at the cellular level, since single fibers and organelles can be resolved and MT dynamics can be accurately measured. Finally, studies in which a protein is removed or knocked out seem more direct than those in which it is overexpressed. If an expected phenotype is not obtained, perhaps a more subtle but nevertheless biologically significant effect may still be identified. It is from this perspective that we attempted to assay a range of MT-related functions in MAP4-depleted cells.

One possibility is that a subset of MTs are particularly affected by MAP4 depletion even if the bulk population is not. It has been shown that acetylated MTs, which correlate with stable MTs, increased dramatically upon tau transfection (Lee and Rock, 1992). Therefore, we tested whether MAP4 is required for acquiring posttranslational modifications of MTs. However, our results showed that the level of posttranslational modifications of MTs was apparently not reduced by removing MAP4 from MTs in the cell. In normal proliferating cells a small population of MAP4-depleted MTs has been demonstrated (Chapin and Bulinski, 1994). Analogous to the MAP4-depleted MTs in Ab-injected cells, the naturally occuring MAP4-depleted MTs are apparently not different in stability or function from MAP4-containing MTs in the same cells.

An important potential function of MAP4, its role in mitosis, was also evaluated in our experiments. At the onset of mitosis, assembly of the mitotic spindle occurs after dissolution of the interphase network of MTs and requires highly dynamic MTs (Belmont et al., 1990). It has been shown that the activity of MPF is sufficient to increase MT dynamics at the onset of mitosis (Verde et al., 1990). Thus, the interphase–mitosis transition of MT dynamics is thought to be induced by phosphorylation reactions mediated by MPF, and by MAP kinase functioning downstream of MPF (Shiina et al., 1992). However, the in vivo substrates of the kinases that are involved in the regulation of MT dynamics have not been identified. One view is that phosphorylation of MAPs alters their ability to stabilize MTs at the interphase to mitosis transition. In fact MAP4 becomes highly phosphorylated in mitosis (Vandré et al., 1991) and phosphorylation of MAP4 by cdc2 kinase in vitro reduces its MT assembly-promoting and -stabilizing activities (Aizawa et al., 1991; Ookata et al., 1995).

Izant et al. (1983) showed that a monoclonal Ab, which presumably bound to HeLa MAP4, when injected into mitotic PtK1 cells before the onset of anaphase inhibited karyokinesis. Although the Ab stained PtK1 spindles, no PtK1 antigen was identified. Therefore, the observed inhibition could have been a result of the Ab acting on an antigenic deterninant shared with MAP4 by another as yet unidentified protein. Furthermore, unlike our polyclonal anti-MAP4, the injected monoclonal Ab bound to the spindle rather than removing the antigen from the spindle. Thus, this mitotic inhibition was the result of an uncharacterized process distinct from the removal of MAP4 that we observe. In our experiments, we tested whether MAP4 was essential for mitosis by using antibody to deplete it from MTs. The result was that the spindle formed and the cells divided even though MAP4 was effectively removed from the spindle; thus, mitotic progression was not dependent on the continued presence of MAP4 on MTs. Nevertheless, in this experiment, we did not address the question of whether or not the phosphorylation of MAP4 by cdc2 kinase plays an active role in mitosis. To test this possibility directly, the phosphorylation sites need to be mapped and mutagenized in such a way as to prevent MAP4 from being phosphorylated.

Additional MT-related functions assayed were possible involvements in organelle transport. The proteins that bind to MTs may be divided into two categories: motor proteins and structural components capable of stabilizing MTs. Whereas MAP4 and the other MAPs have been con-

sidered to be structural MT stabilizing proteins, the molecular motors of the dynein and kinesin superfamilies are members of the motor class. Furthermore, a novel class of CLIPs has been identified that mediates the interaction of cytoplasmic organelles with microtubules (Pierre et al., 1992, 1994). We assayed for possible effects MAP4 removal might have on the MT-dependent distribution of organelles. The presence of MAP4 might be expected to affect interactions of organelles with MT motor proteins; however, no effects were seen on the distribution of organelles known to interact with either plus end– or minus end–directed motors.

Since MAP4 is ubiquitous in proliferating cells, it is hard to believe that it does not have any function. MAP4 may play some role which is beyond our assays. For example, MAP4 may affect the stiffness or spacing of MTs such as has been suggested for MAP2 (Matus, 1994). Although we did not detect any gross alterations of microtubule shape or arrangement in the absence of MAP4, more subtle effects on integrative phenomena such as persistence of directional locomotion or polarity of cell form cannot be excluded. MAP4 may function at certain developmental stages in specific organs or tissues, and be merely expressed gratuitously in cell culture. To test this possibility, transgenic knock-out of the MAP4 gene will be required. Alternatively, some functional redundancy might exist between MAP4 and other MT-associated proteins that play a role in regulating microtubule stability and function. The synthetic lethal approach in cell biology has revealed numerous examples of redundant gene function including aspects of cytoskeletal function (Welch et al., 1994). An additional MAP of 125 kD, named ensconsin (Bulinski and Bossler, 1994), has recently been characterized although its role in microtubule function has yet to be determined. Unlike MAP4, which rapidly dissociates from MTs after the detergent lysis needed to prepare a cytoskeleton, ensconsin remains bound. Evidence of another dilution-insensitive regulatory factor for microtubule stability in fibroblasts has recently been provided (Lieuvin et al., 1994). Possibly, these or other factors serve a function compensatory or partially redundant with MAP4. Further knock-out or deletion experiments will be required to resolve these issues.

We wish to thank Dr. V. I. Rodionov for sharing his knowledge and experience of MAP studies and Drs. P. J. Kronebush, A. B. Verkhovsky, and G. G. Gundersen (Columbia University, New York, NY) for many helpful discussions concerning the experiments. We are especially grateful to Dr. A. B. Verkhovsky for providing the MAP4-tubulin double label results. We also wish to thank Dr. P. G. Wilson for a critical reading of the manuscript.

Supported by National Institutes of Health grant GM 25062 (G. G. Borisy).

Received for publication 3 July 1995 and in revised form 31 October 1995.

References

Aizawa, H., Y. Emori, H. Mirofushi, H. Kawasaki, H. Sakai, and K. Suzuki. 1990. Molecular cloning of a ubiquitously distributed microtubule-associated protein with M_r 190,000. *J. Biol. Chem.* 265:13849–13855.

Aizawa, H., Y. Emori, A. Mori, H. Murofushi, H. Sakai, and, K. Suzuki. 1991. Functional analyses of the domain structure of microtubule-associated protein-U (MAP-U). *J. Biol. Chem.* 266:9841–9846.

Aizawa, H., M. Kamijo, Y. Ohba, A. Mori, K. Okuhara, H. Kawasaki, H. Murofushi, K. Suzuki, and H. Yasuda. 1991. Microtubule destabilization by cdc2/H1 histone kinase: phosphorylation of a "Pro-rich region" in the microtubule-binding domain of MAP4. *Biochem. & Biophy. Res. Commun.* 179: 1620–1626.

Allan, V. J., and T. E. Kreis. 1986. A microtubule-binding protein associated with membranes of the Golgi apparatus. *J. Cell Biol.* 103:2229–2239.

Andersen, S. S. L., B. Buendia, J. E. Dominguez, A. Sawyer, and E. Karsenti. 1994. Effect on microtubule dynamics of XMAP230, a microtubule-associated protein present in *Xenopus Laevis* eggs and dividing cells. *J. Cell Biol.* 127:1289–1299.

Ball, E. H., and S. J. Singer. 1982. Mitochondria are associated with microtubules and not with intermediate filaments in cultured fibroblasts. *Proc. Natl. Acad. Sci. USA.* 79:123–126.

Barlow, S., M. L. Gonzalez-Garay, R. R. West, J. B. Olmsted, and F. Cabral. 1994. Stable expression of heterologous microtubule-associated proteins in chinese hamster ovary cells: evidence for differing roles of MAPs in microtubule organization. *J. Cell Biol.* 126:1017–1029.

Belmont, L. D., A. A. Hyman, K. E. Sawin, and T. J. Mitchison. 1990. Real-time visualization of cell cycle-dependent changes in microtubule dynamics in cytoplasmic extracts. *Cell.* 62:579–589.

Borisy, G. G., J. M. Marcum, J. B. Olmsted, D. B. Murphy, and K. A. Johnson. 1975. Purification of tubulin and associated high molecular weight proteins from porcine brain and characterization of microtubule assembly in vitro. *Ann. NY Acad. Sci.* 253:107–132.

Bradford, M. M. 1976. A rapid and sensitive method for the quantitation of microgram quantities of protein utilizing the principle of protein dye binding. *Anal. Biochem.* 72:248–254.

Bulinski, J. C., and G. G. Borisy. 1979. Self-assembly of Hela tubulin and the identification of Hela microtubule-associated proteins. *Proc. Natl. Acad. Sci. USA.* 76:293–297.

Bulinski, J. C., and G. G. Borisy. 1980*a*. Immunofluorescence localization of Hela cell MAPs on microtubules in vitro and in vivo. *J. Cell Biol.* 87:792–801.

Bulinski, J. C., and G. G. Borisy. 1980*b*. Widespread distribution of a 210,000 mol wt microtubule-associated protein in cells and tissue of primates. *J. Cell Biol.* 87:802–808.

Bulinski, J. C., and A. Bossler. 1994. Purification and characterization of ensconsin, a novel microtubule stabilizing protein. *J. Cell Sci.* 107:2839–2849.

Bulinski, J. C. 1994. MAP4. *In* Microtubules. J. S. Hyams and C. W. Lloyd, editors. Wiley-Liss, New York. 167–182.

Caceres, A., and K. S. Kosik. 1990. Inhibition of neurite polarity by tau antisense oligonucleotides in primary cerebellar neurons. *Nature (Lond.).* 343: 461–463.

Cassimeris, L. U., R. A. Walker, and N. K. Pryer. 1988. Real-time observation of microtubule dynamic instability in living cells. *J. Cell Biol.* 107:2223–2231.

Chapin, S. J., and J. C. Bulinski. 1991. Non-neuronal 210×10^3 M_r microtubule-associated protein 4 (MAP4) contains a domain homologous to the microtubule-binding domains of neuronal MAP2 and tau. *J. Cell Sci.* 98:27–36.

Chapin, S. J., and J. C. Bulinski. 1992. Microtubule stabilization by assembly promoting microtubule-associated proteins: A repeat performance. *Cell Motil. & Cytoskel.* 23:236–243.

Chapin, S. J., C. M. Lue, M. T. Yu, and J. C. Bulinski. 1995. Differential expression of alternatively spliced forms of MAP4: A repertoire of structurally different microtubule-binding domains. *Biochemistry.* 34:2289–2301.

Chen, L. B. 1989. Fluorescent labeling of mitochondria. *In* Methods in Cell Biology. Yu-li Wang and D. Lansing Taylor, editors. Vol. 29. Harcourt Brace Jovanovich, Cleveland, OH. 103–123.

Dingus, J., R. A. Obar, J. S. Hyams, M. Goedert, and R. Vallee. 1991. Use of heat-stable microtubule-associated protein class-specific antibody to investigate the mechanism of microtubule binding. *J. Biol. Chem.* 266:18854–18860.

Dinsmore, J. H., and F. Solomon. 1991. Inhibition of MAP2 expression affects both morphological and cell division phenotypes of neuronal differentiation. *Cell.* 64:817–826.

Drubin, D. G., and M. W. Kirschner. 1986. Tau protein function in living cells. *J. Cell Biol.* 103:2739–2746.

Gundersen, G. G., S. Khawaja, and J. C. Bulinski. 1987. Post-polymerization detyrosination of alpha-tubulin: a mechanism for subcellular differentiation of microtubules. *J. Cell Biol.* 105:251–264.

Harada, A., K. Oguchi, S. Okabe, J. Kuno, S. Terada, T. Ohshima, R. Sato-Yoshitake, Y. Takei, T. Noda, and N. Hirokawa. 1994. Altered microtubule organization in small-calibre axons of mice lacking tau protein. *Nature (Lond.).* 369:488–491.

Hirokawa, N. 1994. Microtubule organization and dynamics dependent on microtubule-associated proteins. *Curr. Opin. Cell Biol.* 6:74–81.

Izant, J. G., J. A. Weatherbee, and J. R. McIntosh. 1983. A microtubule-associated protein antigen unique to mitotic spindle microtubules in PtK1 cells. *J. Cell Biol.* 96:424–434.

Jockusch, B. M., B. Zurk, R. Zahn, A. Westmeyer, and A. Fuchtbauer. 1991. Antibodies against vertebrate microfilament proteins in the analysis of cellular motility and adhesion. *J. Cell Sci. Suppl.* 14:41–47.

Kanai, Y., R. Takemura, T. Oshima, H. Mori, Y. Ihara, M. Yanagisawa, T. Masaki, and N. Hirokawa. 1989. Expression of multiple tau isoforms and microtubule bundle formation in fibroblasts transfected with a single tau cDNA. *J. Cell Biol.* 109:1173–1184.

Khawaja, S., G. G. Gundersen, and J. C. Bulinski. 1988. Enhanced stability of microtubules enriched in detyrosinated tubulin is not a direct function of the detyrosination level. *J. Cell Biol.* 93:576–582.

Laemmli, U.K. 1970. Cleavage of structural proteins during the assembly of the

head of bacteriophage T4. *Nature (Lond.).* 227:680–685.
Lee, G., N. Cowan, and M. Kirschner. 1988. The primary structure and heterogeneity of tau protein from mouse brain. *Science (Wash. DC).* 239:285–288.
Lee, G., and S. L. Rook. 1992. Expression of tau protein in non-neuronal cells: microtubule binding and stabilization. *J. Cell Sci.* 101:227–237.
Lewis, S. A., D. Wang, and N. J. Cowan. 1988. Microtubule-associated protein MAP2 shares a microtubule binding motif with tau protein. *Science (Wash. DC).* 242:936–939.
Lewis, S. A., I. E. Vanov, G. H. Lee, and N. J. Cowan. 1989. Microtubule organization in dendrites and axons is determined by a short hydrophobic zipper in microtubule-associated proteins MAP2 and tau. *Nature (Lond.).* 342:498–505.
Lieuvin, A., J. Labbé, M. Dorée, and D. Job. 1994. Intrinsic microtubule stability in interphase cells. *J. Cell Biol.* 124:985–996.
Mangeat, P. H., and K. Burridge. 1984. Immunoprecipitation of nonerythrocyte spectrin within live cells following microinjection of specific antibodies: relation to cytoskeletal structures. *J. Cell Biol.* 98:1363–1377.
Matus, A. 1994. MAP2. *In* Microtubules. J. S. Hyams and C. W. Lloyd, editors. Wiley-Liss, New York. 155–166.
Mitchison, T. J., and M. W. Kirschner. 1984. Dynamic instability of microtubule growth. *Nature (Lond.).* 312:237–247.
Nuckolls, G. H., L. H. Romer, and K. Burridge. 1992. Microinjection of antibodies against talin inhibits the spreading and migration of fibroblasts. *J. Cell Sci.* 102:753–762.
Olmsted, J. B., D. L. Stemple, W. M. Saxton, B. W. Neighbors, and J. R. McIntosh. 1989. Cell cycle-dependent changes in the dynamics of MAP2 and MAP4 in cultured cells. *J. Cell Biol.* 109:211–223.
Olmsted, J. B. 1991. Non-motor microtubule-associated proteins. *Curr. Opin. Cell Biol.* 3:52–58.
Ookata, K., S. Hisanaga, J. C. Bulinski, H. Murofushi, H. Aizawa, T. J. Itoh, H. Hotani, E. Okumura, K. Tachibana, and T. Kishimoto. 1995. Cyclin B interaction with microtubule-associated protein 4 (MAP4) targets $p34^{cdc2}$ kinase to microtubules and is a potential regulator of M-phase microtubule dynamics. *J. Cell Biol.* 128:849–862.
Pagano, R. E. 1989. A fluorescent derivative of ceramide: physical properties and use in studying the Golgi apparatus of animal cells. *In* Methods in Cell Biology. Y. L. Wang and D. L. Taylor, editors. Vol. 29. Harcourt Brace Jovanovich, Cleveland, OH. 75–85.
Pereira, A., J. Doshen, E. Tanaka, and L. S. B. Goldstein. 1992. Genetic analysis of a Drosophila microtubule-associated protein. *J. Cell Biol.* 116:377–383.
Pierre, P., J. Scheel, J. E. Rickard, and T. E. Kreis. 1992. CLIP-170 links endocytic vesicles to microtubules. *Cell.* 70:887–900.
Pierre, P., R. Pepperkok, and T. E. Kreis. 1994. Molecular characterization of two functional domains of CLIP-170 in vivo. *J. Cell Sci.* 107:1909–1920.
Piperno, G., M. LeDizet, and X. J. Chang. 1987. Microtubules containing acetylated alpha-tubulin in mammalian cells in culture. *J. Cell Biol.* 104:289–302.
Sammak, P. J., and G. G. Borisy. 1988. Direct observation of microtubule dynamics in living cells. *Nature (Lond.).* 332:724–726.
Saxton, W. M., D. L. Stemple, R. J. Leslie, E. D. Salmon, M. Zavortink, and J. R. McIntosh. 1984. Tubulin dynamics in cultured mammalian cells. *J. Cell Biol.* 99:2175–2186.
Schulze, E., and M. Kirschner. 1986. Microtubule dynamics in interphase cells. *J. Cell Biol.* 102:1020–1031.
Schulze, E., and M. Kirschner. 1987. Dynamic and stable populations of microtubules in cells. *J. Cell Biol.* 104:277–288.
Shiina, N., T. Moriguchi, E. Ohta, Y. Gotoh, and E. Nishida. 1992. Regulation of a major microtubule associated protein by MPF and MAP kinase. *EMBO J.* 11:3977–3984.
Smith, D. B., and K. S. Johnson. 1988. Single-step purification of polypeptides expressed in Escherichia coli as fusion with glutathione S-transferase. *Gene.* 67:31–40.
Soltys, B. J., and G. G. Borisy. 1985. Polymerization of tubulin in vivo: direct evidence for assembly onto microtubule ends and from centrosomes. *J. Cell Biol.* 100:1682–1689.
Towbin, H., T. Staehelin, and J. Gordon. 1979. Electrophoretic transfer of proteins from polyacrylamide gels to nitrocellulose sheets: procedure and some applications. *Proc. Natl. Acad. Sci. USA.* 76:4350–4354.
Vallee, R. B., and G. G. Borisy. 1978. The non-tubulin component of microtubule protein oligomers: effect on self-association and hydrodynamic properties. *J. Biol. Chem.* 253:2834–2845.
Vandenbunder, B., and G. G. Borisy. 1986. Decoration of microtubules by fluorescently labeled microtubule-associated protein 2 (MAP2) does not interfere with their spatial organization and progress through mitosis in living fibroblasts. *Cell Motil. & Cytoskel.* 6:570–579.
Vandré, D. D., V. E. Centonze, J. G. Peloquin, R. M. Tombes, and G. G. Borisy. 1991. Proteins of the mammalian mitotic spindle: phosphorylation/dephosphorylation of MAP4 during mitosis. *J. Cell Sci.* 98:577–588.
Verde, F., J. Labbe, M. Doree, and E. Karsenti. 1990. Regulation of microtubule dynamics by cdc2 protein kinase in cell-free extracts of Xenopus eggs. *Nature (Lond.).* 343:233–238.
Weatherbee, J. A., R. B. Luftig, and R. R. Weihing. 1980. Purification and reconstitution of Hela microtubules. *Biochemistry.* 19:4116–4123.
Webster, D. R., G. G. Gundersen, J. C. Bulinski, and G. G. Borisy. 1987. Differential turnover of tyrosinated and detyrosinated microtubules. *Proc. Natl. Acad. Sci. USA.* 94:9040–9044.
Webster, D. R., J. Wieland, K. Weber, and G. G. Borisy. 1990. Detyrosination of alpha tubulin does not stabilize microtubules in vivo. *J. Cell Biol.* 111:113–122.
Welch, M. D., D. A. Holtzman, and D. G. Drubin, 1994. The yeast actin cytoskeleton. *Curr. Opin. Cell Biol.* 6:110–119.
West, R. R., K. M. Tenbarge, and J. B. Olmsted. 1991. A model for microtubule-associated protein 4 structure. *J. Biol. Chem.* 266:21886–21896.
Zhai, Y., and G. G. Borisy. 1994. Quantitative determination of the proportion of microtubule polymer during the mitosis-interphase transition. *J. Cell Sci.* 107(4):881–890.
Zhai, Y., P. J. Kronebusch, and G. G. Borisy. 1995. Kinetochore microtubules dynamics and the metaphase–anaphase transition. *J. Cell Biol.* 131:721–734.